# 核医学における肝線維化の評価に関する研究

# Liver fibrosis assessment using $^{99m}$Tc-GSA SPECT/CT fusion imaging

所谷　亮太朗

鈴鹿医療科学大学大学院 医療科学研究科 医療科学専攻
博士（医療科学）の学位申請論文

指導教員　　安田　鋭介　教授

２０２１年３月

博　士　論　文　審　査　委　員

主査　　柴田　幸一　教授

副査　　栃谷　史郎　准教授

副査　　中舎　幸司　助教

<h1 align="center">Liver fibrosis assessment using $^{99m}$Tc-GSA SPECT/CT fusion imaging.</h1>

<p align="center">医療科学専攻　　所谷　亮太朗</p>

<p align="center">(指導教員 ： 安田　鋭介　教授)</p>

## 【はじめに】

　肝障害が進行すると肝実質の線維化が進行するため、肝線維化は肝障害の重症度を表す重要な指標である。肝線維化が進行すると肝硬変へと移行するが、肝硬変症例に対する肝切除は出血、肝不全のリスクが高く、許容される切除体積も小さい。従って肝切除術前に背景肝の線維化の程度を評価する事は、治療方針を決定する上で非常に重要である。肝臓の線維化の有無を調べる方法として肝生検、ヒアルロン酸、タイプ III プロコラーゲン–N–ペプチド(PIIIP)、4 型コラーゲンなどがあるが、その重症度を非侵襲的に判断する有用な指標は確立されていない。今回我々は Tc-99m-diethylenetriamine-penta-acetic acid- galactosyl human serum albumin ($^{99m}$Tc-GSA) scintigraphy を用いて肝線維化の重症度が測定できないか検討を行った。 これらの報告の多くは GSA シンチグラフィ由来の指標である LHL15、HH15 を使用して検討を行っている。しかしながら LHL15 や HH15 は Planar 撮像により算出されているため、深さ方向の情報に乏しく、正確性に欠けるという欠点が指摘されている。

　近年、シンチグラフィの分野において、SPECT-CT による減弱・散乱補正・分解能補正の高精度化により、これまで非定量的とされてきた SPECT 検査の SUV を用いた定量化が報告されている。 SUV は放射性薬剤の臓器への集積の強さを表す指標であり、深さ方向の情報を有している。

## 【目的】

　我々は SUV の概念を $^{99m}$Tc-GSA シンチグラフィに適応し、肝臓全体の SUVmean を測定した。本研究では血液検査所見、$^{99m}$Tc-GSA 検査由来の LHL15、SUVmean のいずれが最も実際の肝線維化の重症度と相関するか検討した。

## 【方法】

　対象は高知医療センターで 2014 年 9 月から 2017 年 9 月の間に肝切除術を受けた 86 例であり、全例術前に $^{99m}$Tc-GSA SPECT/CT fusion imaging を受けていた。肝機能指標として術前の Platelets($\times 10^4$/mm$^3$)、Total bilirubin(g/dL)、Prothrombin time(%)、Albumin(g/dL)を調べた。採血は全て術前の一週間以内に行われた。我々は研究にあたり施設内倫理審査委員会の認証(161007)を得た。

　方法は得られた SUVmean と肝臓の線維化を表す指標、LHL15、Albumin(g/dL)、Total bilirubin(g/dL)、Platelets($\times 10^4$/mm$^3$)、Prothrombin time(%)の 6 つの指標に対して線維化の程度を評価した。線維化の程度は腫瘍から離れた組織の切除標本から病理医により診断された。切除標本の組織学的分類は、新犬山分類を使用して分類された。切除標本は、F0(線維化なし)、F1(門脈域の線維化性拡大)、F2(線維性架橋形成)、F3(小葉のひずみを伴う線維性架橋形成)、F4(肝硬変)と 5 段階のスケールで分類された。その際、F0、F1、F2 は非線維化群、F3、F4 は線維化群として分け評価した。$^{99m}$Tc-GSA 静注後 20 分から 28 分の SPECT image を使用して SUVmean を算出した。算出に際しては SUV 算出アプリケーション GI-BONE にて、全肝臓を含むように Volume of Interest(VOI)を設置した。なお、VOI は GI-BONE にて自動的に設定される。

<p align="center">2</p>

【結果】

　血液検査における Albumin(g/dL)、Total bilirubin(g/dL) 、Platelets(×10⁴/mm³)、Prothrombin time(%)の中央値は非線維化群と線維化群でそれぞれ 4.2 vs 3.9 (p=0.272)、0.6 vs 0.7 (p=0.057)、17.6 vs 12.9 (p<0.001)、96.5 vs 86.7 (p=0.008)であり、Platelets、Prothrombin time に有意な差を認めた。
GSA scintigraphy 由来の肝機能指標である LHL15、SUVmean の中央値は非線維化群と線維化群で 0.917 vs 0.874 (p=0.001)、6.8 vs 6.0 　(p<0.001)であり、有意差を認めた。

　単変量解析で有意差を認めた Platelets、Prothrombin time、LHL15 及び SUVmean を多変量解析にて評価した結果、Prothrombin time 及び SUVmean が肝臓線維化の因子であった。
ROC 解析では、重度肝線維症を予測するための SUVmean、Platelets、LHL15、Prothrombin time の AUC 値はそれぞれ 0.804、0.730、0.717、0.668 であった。

【考察】

　肝障害の原因は肝炎ウイルス、アルコール、脂肪肝など様々な原因があるが、肝障害が持続する事により線維化が進行し肝硬変へと移行する。肝硬変例に対する肝切除術は出血、肝不全のリスクが高く、術前に肝線維化の程度を判定することは重要である。肝線維化の評価は肝生検が gold standard ではあるが、侵襲的でありサンプリングエラー、観察者間での診断のバラツキなどの問題がある。非侵襲的に全肝の肝線維化を評価する方法はいまだ確立されていない。

　今回我々は肝線維化の評価に GSA シンチが応用できないか検討した。⁹⁹ᵐTc-GSA は肝細胞表面に存在する肝受容体に特異的に集積し、その集積は肝機能を表す。よって ⁹⁹ᵐTc-GSA は直接的に肝臓の線維化を評価する薬剤ではないが、肝臓の先行論文では Okabe らは、15 分でのインドシアニングリーンの保持率（ICG R15）と、LHL15 における取り込みの比を用いた肝機能の分類システムを使用して、肝切除後の予備能を予測し、結論として LHL15 は、組織学的肝線維症を予測することで、この分類に貢献できると報告した。しかし、これらの報告は planar 撮像での LHL15 を使用しており、Planar 撮像では深さの情報を有しておらず、正確な評価が困難である場合がある。さらに、⁹⁹ᵐTc-GSA SPECT-CT　Fusion による評価では、LUV や hepatic clearance（HC）といった肝臓の線維化を評価する報告がある。しかし、これらの指標の多くは難解であり、実用的でない場合が多く広く普及しているとは言い難い。

　今研究では評価に SUVmean を使用した。近年では SPECT の補正機能や再構成アルゴリズムの進化により PET 同様に SUV による評価が行えると報告されている。肝線維化評価に SUV を用いる事で、投与量、体重といったパラメータを検査ごとに補正し、定量的な評価が可能となる。SUVmean はすでに PET で広く日常的に用いられている指標であり、算出方法も簡便で、各種ワークステーションやアプリケーションで算出できる。また、GI-BONE ではあらかじめしきいを設定すれば、手動で VOI を設定する必要がなく、術者間のばらつきがない。非線維化群及び線維化群における肝機能指標との比較、検討を多変量解析にて検討したところ、SUVmean に有意差が認められた。この事より SUVmean を用いた肝線維化の評価は、線維化の程度を予測する有用な方法である事が示唆された。

【結論】

⁹⁹ᵐTc-GSA より得られる肝臓の SUVmean は肝線維化の指標となる可能性が示唆された。

DH18101　所谷亮太朗

# 目　　次

DH18101　所谷亮太朗

## Introduction

Degree of fibrosis is an important indicator of liver function, as damage to the organ leads to fibrotic change in the liver parenchyma. Cirrhosis represents the most advanced stage of liver fibrosis, which is associated with a potential risk of malnutrition, coagulopathy, and fatal liver failure, thereby posing restrictions in performing invasive therapeutic procedures [1-4]. Therefore, assessment of the degree of fibrosis is important to decide the treatment strategy for patients with liver diseases. The gold standard of assessment of liver fibrosis is biopsy; however, a non-invasive substitute diagnostic modality has not been established.

Tc-99m-diethylenetriamine-penta-acetic acid-galactosyl human serum albumin ($^{99m}$Tc-GSA) single-photon emission computed tomography (SPECT)/CT fusion imaging has been routinely used in the evaluation of whole and regional liver functions prior to hepatectomy at this institution [5]. The present study investigated the potential utility of the technique in the evaluation of liver fibrosis. $^{99m}$Tc-GSA is exclusively taken up by the liver and specifically binds to asialoglycoprotein receptor on hepatocytes and decreased number of receptors are observed in patients with liver damage [6-7]. Therefore, $^{99m}$Tc-GSA scintigraphy enables the direct estimation of functioning hepatocytes and is an excellent method for the evaluation of regional and whole liver function [8].

These previous reports used the ratio of liver to heart-plus-liver radioactivity for 15 minutes ($LHL_{15}$) value, which is representative whole liver function index of 99mTc-GSA scintigraphy; one previous report described that $LHL_{15}$ value showed significant correlation with the degree of liver fibrosis [9]. However, $LHL_{15}$ is detected by planar image of $^{99m}$Tc-GSA scintigraphy; therefore, is deficient in the three-dimensional depth direction information (Fig. 1a) [10].

A recent study reported highly accurate attenuation correction, scatter correction, and resolution correction to enable the quantification using standardized uptake value (SUV) [11]. SUV depicts the degree of accumulation of radiopharmaceutical substances in the target organ, and enables obtaining three-dimensional depth direction information [12]. Therefore, it was assumed that SUV might demonstrate better correlation with liver fibrosis than $LHL_{15}$. The concept of SUV was applied to 99mTc-GSA scintigraphy for the first time in this study, and the value of this indicator was investigated in the evaluation of liver fibrosis.

## Methods
### Patients

Eighty-six patients who underwent hepatectomy between September 2014 and September 2017 were enrolled in the retrospective study. All patients underwent $^{99m}$Tc-GSA SPECT/CT fusion imaging prior to the hepatectomy to evaluate whole and regional liver functions. The study was approved by the institutional review board, with waiver of informed consent.

### Blood biochemistry (Liver function tests)

The values of four blood biochemical indices (albumin, total bilirubin, platelet count, and prothrombin time activity) prior to the hepatectomy were investigated.

### $^{99m}$Tc-GSA SPECT/CT fusion imaging

$^{99m}$Tc-GSA SPECT/CT fusion imaging has been routinely applied at our institution, in hepatectomy candidates to evaluate liver function. All patients underwent the examination with a Symbia T6 scanner (Siemens, Munich, Germany). This instrument combines variable angle dual detector SPECT with 6-slice CT for rapid, accurate attenuation correction and precise localization. The instrument also enables the seamless transition from a SPECT

5

examination to a CT examination, and both SPECT and CT images could be obtained in a single examination without the need for change in position. The procedure of the investigation was as follows. After overnight fasting, the patient was placed in a supine position. Cardiac and respiratory synchronization were not used in this modality. Instead, to minimize the possibility of occurrence of artefacts due to cardiac pulsation and respiratory motion, the patients were encouraged to rest and take a small, slow breath before image acquisition. 99mTc-diethylenetriamine-penta-acetic acid-GSA (Nihon Medi- Physics, Tokyo, Japan) (185 MBq/3 mg) was injected into an antecubital vein. SPECT data acquisition (60 steps of 20 s/step, 360°, 128 × 128 matrix) was started 20 min after the injection with a low-energy, high-resolution collimator; the entire study duration was approximately 30 min. The reconstruction algorithm for SPECT was 3-dimensional ordered subset expectation maximization (iteration,10; subsets,6), with attenuation and scatter corrections. 3D Gaussian filter was used as a post processing filter (9.6 mm full-width at half-maximum). Following SPECT examination, non-enhanced CT images were obtained under standard conditions of 130 kV, 345 mA, 12 mm table feed per rotation, 0.6-s gantry rotation time, 0.6-mm collimation, and 1-mm reconstruction. CT images were reconstructed using a standard algorithm with a 166-cm field-of-view of the target sites. The SPECT and CT images were fused automatically using the embedded Siemens common platform software Syngo MI workplace. SPECT slice data were retrieved through Digital Imaging and Communications in Medicine (DICOM), and SPECT slices were converted to a CT-like data volume for the fusion of the SPECT and CT images.

**Calculation of LHL$_{15}$**

The ROI was set by one radiological technologist and one radiologist specializing in nuclear medicine at this information on mutual consent. The LHL$_{15}$ value was calculated by dividing the radioactivity of the liver ROI (L$_{15}$) by the sum of the radioactivity of the liver and heart ROIs (L$_{15}$+H$_{15}$) at 15 min post-injection (Fig. 1a) [13-14]:
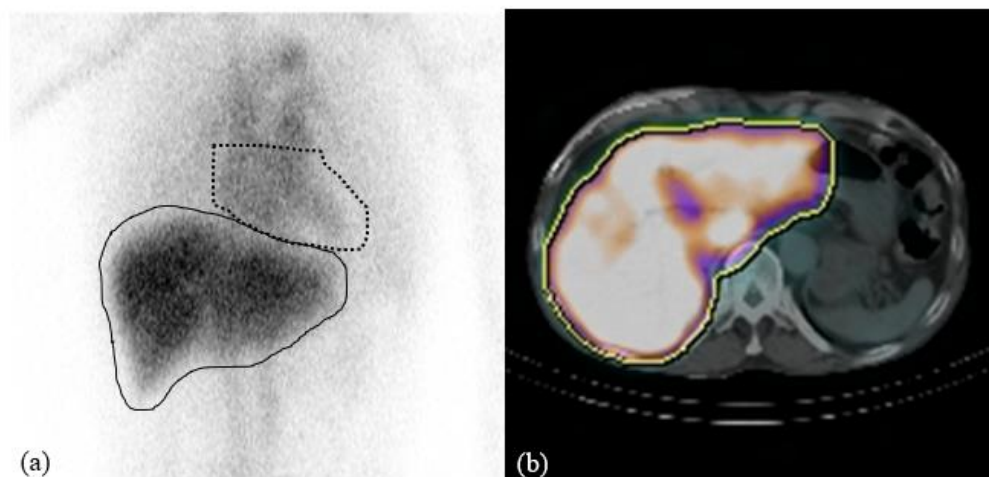


Fig. 1

$$LHL_{15} = \frac{L15}{L15+H15}$$

DH18101　所谷亮太朗

**Calculation of SUV$_{mean}$**

 The accumulation of 99mTc-GSA in the liver was evaluated using SUV [11]. Decay correction was applied in all patients to control the fluctuation at the start time of the acquisition. SUV value was normalized by the liver volume, which was calculated automatically using workstation VINCENT (FUJIFILM, Tokyo, Japan) [15].

SUV was calculated using the following formula:

$$SUV_{mean} = \frac{\text{Radioactivity of liver VOI (Bq/ml)}}{\text{Dose at the start of scan(Bq)/Livervolume (ml)} \times 10}$$

 Setting the volume of interest (VOI) at the site of 99mTc-GSA accumulation in the liver is necessary to calculate SUV; therefore, we applied a commercially available GI-BONE (AZE Co., Ltd., Tokyo, Japan), which is known to set VOI automatically (Fig. 1b). The VOI was placed to contain the whole liver. Then, the software automatically detected the region of voxel with SUV > 3, and the mean value of SUV in the designated region was calculated. Further, 99mTc-GSA is taken up only in the liver, not in whole body, and therefore, liver volume was utilized to normalize the radioactivity in this study.

**Degree of fibrosis**

 Degree of fibrosis was pathologically diagnosed in the liver parenchyma apart from the liver tumor in each resected specimen. The Ludwig scale was utilized to stratify the grade of fibrosis; F1 (No fibrosis or fibrosis confined to enlarged portal tracts), F2 (periportal fibrosis or portal-to-portal septa but intact architecture), F3 (septal fibrosis with architecture distortion), and F4 (probable or definite cirrhosis). The degree of fibrosis was assessed by two pathologists who were blinded the patient characteristics. Grades F1 and F2 were classified in the Non-fibrosis group, and grades F3 and F4 were classified in the Fibrosis group [16]. Univariate and multivariate analysis were performed between the two groups on four blood biochemical indices and two [99mTc]-GSA scintigraphy derived liver function indices to evaluate the independent predictive value for severe fibrosis. The diagnostic value of the index for severe fibrosis was assessed by calculating the area under the receiver operating characteristics (ROC) curve.

**Statistical analysis**

 The data were not distributed normally. Therefore, median values and non-parametric statistical testing procedures were utilized. The Mann–Whitney U test was used for continuous variables, and the chi-square test was used for categorical variables. Differences between medians were considered statistically significant at p value of < 0.05. Significant variables obtained by univariate analysis were entered simultaneously (forced entry method) into multivariate logistic regression analysis to evaluate their independent predictive value for severe fibrosis. The diagnostic value of the index was assessed by calculating the area under the ROC curve. These statistical analyses were performed using SPSS 24 for Windows (SPSS, Chicago, IL, United States).

**RESULTS**

**Clinical characteristics**

 The clinical characteristics of the patients included in this study (n=86) are described in Table 1. The patient

DH18101　所谷亮太朗

population comprised of 36 males and 15 females with a median age of 72 years (range, 42–86 years) in the Non-fibrosis group. The Fibrosis group comprised 25 males and 10 females with a median age of 74 years (range, 39–86 years), and no significant differences were observed between the two groups (Table 1). The body weights in both groups were also equivalent. The positive rates of hepatitis B, hepatitis C, alcohol abuse, and non-alcoholic steatohepatitis showed no significant differences between the two groups (Table 1).

**Table 1** Clinical characteristics of the non-fibrosis and fibrosis groups

| | Non-fibrosis ($n=51$) | Fibrosis ($n=35$) | $p$ value |
|---|---|---|---|
| Gender (male/ female) | 36/15 | 25/10 | 0.868 |
| Age range (median) | 42–86 (72) | 39–86 (74) | 0.786 |
| Body weight (kg) | 56.15 | 58.5 | 0.876 |
| Hepatitis B ($\pm$) | 8/43 | 4/31 | 0.542 |
| Hepatitis C ($\pm$) | 11/40 | 12/23 | 0.135 |
| Alcohol abuse ($\pm$) | 8/43 | 6/29 | 0.831 |
| NASH ($\pm$) | 1/50 | 3/32 | 0.162 |

*NASH* non-alcoholic steatohepatitis

**Comparison of liver function index between Non- fibrosis and Fibrosis groups**

Results of univariate and multivariate analyses have been summarized in Table 2. In univariate analysis, the median value of serum albumin (g/dL), total bilirubin (g/dL), platelet count ($\times 10^4/\text{mm}^3$), and prothrombin time activity (PT%) were 4.2 vs. 3.9 ($p = 0.272$), 0.6 vs. 0.7 ($p = 0.057$), 17.6 vs. 12.9 ($p < 0.001$), and 96.5 vs. 86.7 ($p = 0.009$), respectively between the Non-fibrosis and Fibrosis groups. The platelet count and PT% showed significant differences between the two groups. The median value of $LHL_{15}$ and $SUV_{mean}$ were 0.917 vs. 0.874 ($p<0.001$) and 6.8 vs. 6.0 ($p<0.001$), respectively, and both the 99mTc-GSA scintigraphy derived indices showed significant differences between the two groups. In these indices, multivariate analysis showed that PT% (OR: 0.519), $LHL_{15}$ (OR: 0.513) and SUV mean (OR: 0.168) significantly correlated with liver fibrosis.

**Table 2** Comparison of liver function index between the non-fibrosis and fibrosis groups

| | Univariate | | | Multivariate | |
|---|---|---|---|---|---|
| | Non-fibrosis | Fibrosis | $p$ value | Odds ratio | $p$ value |
| Albumin (g/dL) | 4.2 (3.0–5.0) | 3.9 (2.3–4.9) | 0.272 | | |
| Total bilirubin (mg/dL) | 0.6 (0.2–1.2) | 0.7 (0.3–1.7) | 0.057 | | |
| Platelet count ($\times 10^4/\text{mm}^3$) | 17.6 (6.9–49.6) | 12.9 (6.5–42.9) | < 0.001 | 0.625 (0.313–1.222) | 0.166 |
| Prothrombin time (%) | 96.5 (33.6–117.7) | 86.7 (51.5–117.7) | 0.009 | 0.519 (0.258–0.824) | 0.020 |
| $LHL_{15}$ | 0.917 (0.786–0.960) | 0.874 (0.687–0.950) | < 0.001 | 0.513 (0.278–0.947) | 0.038 |
| $SUV_{mean}$ | 6.8 (5.1–8.1) | 6.0 (3.2–7.1) | < 0.001 | 0.168 (0.048–0.435) | < 0.001 |

Number in non-fibrosis and fibrosis groups shows the median value. Number in the parentheses shows range of the value

**Diagnostic value of indices for liver fibrosis**

ROC curves were constructed and AUCs were compared on four variables: platelet count, PT%, LHL15, and $SUV_{mean}$ (Fig. 2). The AUCs were 0.804 for $SUV_{mean}$, 0.730 for platelet count (vs. $SUV_{mean}$, $p = 0.249$), 0.717 for LHL15 (vs. $SUV_{mean}$, $p = 0.084$), and 0.668 for PT% (vs. $SUV_{mean}$, $p = 0.075$). Although statistical significances of AUCs were not observed between $SUV_{mean}$ and other 3 variables, $SUV_{mean}$ showed the largest AUC. The optimal cut-off value for $SUV_{mean}$ was 6.7, which yielded 62.9% sensitivity, 96.9% specificity, 97.1% positive predictive
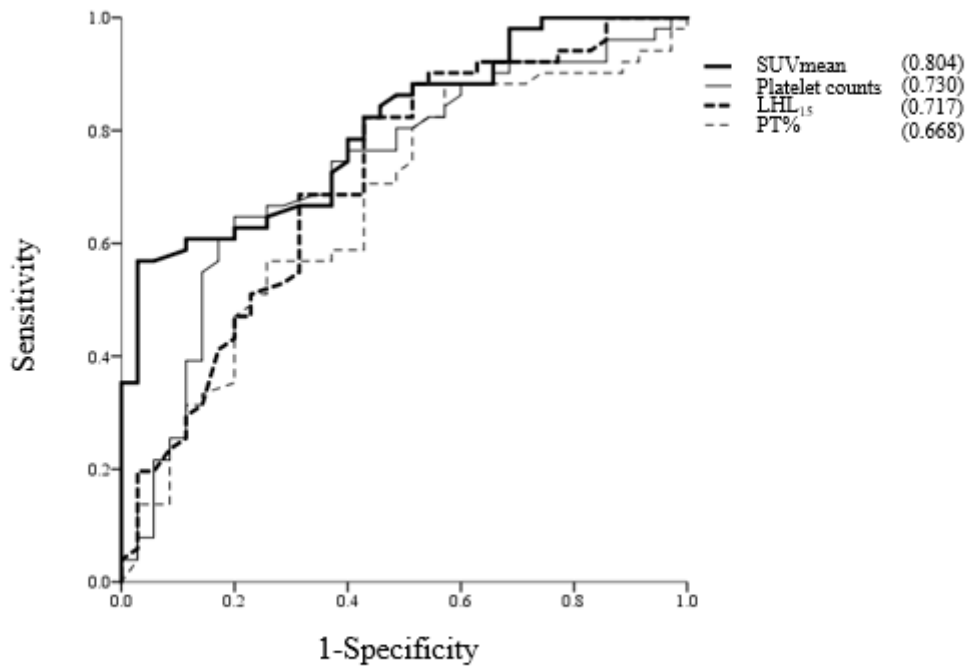
8

value, and 60.8% negative predictive value.



Fig. 2

**Discussion**

Continuous damage to the liver leads to progression of fibrosis and eventually cirrhosis, regardless of the cause of liver damage such as hepatitis virus, alcohol, and fatty liver [3]. Patients with cirrhosis have a potential risk of fatal liver failure; therefore, assessment of fibrosis is crucial to decide the treatment strategy for patients with liver diseases. Liver biopsy, which is the gold standard for assessing fibrosis, is an invasive technique and is associated with limitations such as bleeding and/or sampling error [17]. Non-invasive indicators such as hyaluronic acid, procollagen III peptide, and type IV collagen [18-22], are effective markers of fibrosis; however, these markers are not specific to the liver.

Therefore, the present study investigated the utility of $^{99m}$Tc-GSA scintigraphy in the evaluation of liver fibrosis. A previous study reported that $LHL_{15}$ value of $^{99m}$Tc-GSA scintigraphy showed significant correlation with the degree of liver fibrosis [9]. However $LHL_{15}$ lacks the three-dimensional depth direction information, as the index is calculated from planar scintigraphic images, which do not accurately reflect hepatocyte volume. To overcome this problem, SUV was applied in $^{99m}$Tc-GSA scintigraphy for the first time in this study. The concept of SUV is widely applied and commonly used in the field of positron emission tomography scan, and the quantified value facilitates evaluation of the target organ. SUV could be accurately and automatically measured from $^{99m}$Tc-GSA SPECT/CT fusion imaging by using GI-BONE.

Several liver function indices were compared between the Fibrosis and Non-fibrosis groups in this study. Multivariate analysis revealed that PT%, $LHL_{15}$, and $SUV_{mean}$ showed significant discrepancies between the two groups, and the OR was smallest in $SUV_{mean}$. Further, ROC curve revealed that $SUV_{mean}$ was the most accurate index for diagnosing severe fibrosis. This significant correlation between $SUV_{mean}$ and liver fibrosis was estimated

9

to be attributed to the following reasons: 1. $^{99m}$Tc-GSA has the specific nature of being taken up exclusively by the liver, and the decrease in number of functioning hepatocytes due to severe fibrosis was reflected as decreased accumulation of $^{99m}$Tc-GSA in the liver, and 2. Accurate assessment of 99mTc-GSA accumulation in the liver was obtained by applying SUV.

Despite of the apparent utility of SUV in assessing liver fibrosis, this study has a number of limitations. The major drawback of $^{99m}$Tc-GSA scintigraphy is that, this modality evaluates the functioning hepatocytes, and is not a direct technique to evaluate liver fibrosis. Therefore, further investigations are necessary to elucidate the mechanism of the strong correlation of liver fibrosis and $SUV_{mean}$ of $^{99m}$Tc-GSA scintigraphy. Second, there is no clinical availability of $^{99m}$Tc-GSA in Western countries, although many studies have been published using this radiopharmaceutical agent in Japan and some countries. Third, the correlation between $SUV_{mean}$ and long-term prognosis was estimated to enhance the clinical utility of this study. However, we could not investigate the correlation, because 86 patients in this study were candidates for hepatectomy, and the prognoses were strongly influenced by each hepatic tumor.

In conclusion, $SUV_{mean}$ of $^{99m}$Tc-GSA scintigraphy enables highly accurate prediction of severe liver fibrosis.

### References

1. Farges O, Malassagne B, Flejou J.F, Balzan S, Sauvanet.A, Belghiti J. Risk of major liver resection in patients with underlying chronic liver disease: a reappraisal. Ann Surg. 1999;229: 210-5.

2. Nagino M, Kamiya J, Nishio H, Ebata T, Arai T, Nimura Y. Two hundred forty consecutive portal vein embolizations before extended hepatectomy for biliary cancer: surgical outcome and long-term follow-up. Ann Surg. 2006;243:364-72.

3. Zarzavadjian A, Bian L, Costi R, Sbai-Idrissi M.S, Smadja C. Liver resection and metabolic disorders: an undescribed mechanism leading to postoperative mortality. World J Gastroenterol. 2014;20:55-62.

4. Wang Q, Fiel M, Blank S, Luan W, Kadri H, Kim K.W, et al. Impact of liver fibrosis on prognosis following liver resection for hepatitis B-associated hepatocellular carcinoma. Br J Cancer. 2013;109:573-81.

5. Sumiyoshi T, Shima Y, Okabayashi T, Noda Y, Hata Y, Murata Y, et al. Functional Discrepancy between Two Liver Lobes after Hemilobe Biliary Drainage in Patients with Jaundice and Bile Duct Cancer: An Appraisal Using 99mTc-GSA SPECT/CT Fusion. Radiology. 2014;273:444-51.

6. Sobue G, Kosaka A. Asialoglycoproteinemia in a case of primary hepatic cancer. Hepatogastroenterology. 1980;27:200-3.

7. Marshall JS, Green AM, Pensky J, Williams S, Zinn A, Carlson DM. Measurement of circulating desialylated glycoproteins and correlation with hepatocellular damage. J Clin Invest. 1974;54:555-62.

8. Okabayashi T, Shima Y, Morita S, Shimada Y, Sumiyoshi T, Sui K, et al. Liver Function Assessment Using Technetium 99m-Galactosyl Single-Photon Emission Computed Tomography/CT Fusion Imaging: A Prospective Trial. J Am Coll Surg. 2017;225;789-97.

9. Okabe H, Beppu T, Hayashi H, Mima K, Nakagawa S, Kuroki H, et al. Rank classification based on the combination of indocyanine green retention rate at 15 min and (99m) Tc-DTPA-galactosyl human serum albumin scintigraphy predicts the safety of hepatic resection. Nucl Med Commun. 2014;35:478-83.

10. Hasegawa D, Onishi H. Evaluation of Accuracy for Quantitative Predictor of Hepatic Functional Reserve Using Planar and SPECT Images in the 99mTc-GSA Scintigraphy, Nihon Hoshasen Gijutsu Gakkai Zasshi. 2017;73:1055–60.

DH18101　所谷亮太朗

11. Suh MS, Lee WW, Kim YK, Yun PY, Kim SE. Maximum Standardized Uptake Value of 99mTc Hydroxymethylene Diphosphonate SPECT/CT for the Evaluation of Temporomandibular Joint Disorder. Radiology. 2016;280:890-6.

12. Kinahan PE, Fletcher JW. Positron emission tomography-computed tomography standardized uptake values in clinical practice and assessing response to therapy. Semin Ultrasound CT MR. 2010;31:496-505.

13. Kokudo N, Vera DR, Makuuchi M. Clinical application of TcGSA. Nucl Med Biol. 2003;30:845-9.

14. Kwon AH, Ha-Kawa SK, Uetsuji S, Kamiyama Y, Tanaka Y. Preoperative regional maximal removal rate of technetium-99m- galactosyl human serum albumin (GSA-Rmax) is useful for judging the safety of hepatic resection. Surgery. 1995;117:429–34.

15. Oshiro Y, Ohkohchi N. Three-Dimensional Liver Surgery Simulation: Computer-Assisted Surgical Planning with Three-Dimensional Simulation Software and Three-Dimensional Printing. Tissue Eng Part A. 2017;23:474-80.

16. Ludwig J. The nomenclature of chronic active hepatitis ; An obituary. Gastroenterology. 1993;105 274-8.

17. Vallet-Pichard A, Mallet V, Nalpas B, Verkarre V, Nalpas A, Dhalluin-Venier V, et al. FIB-4: an inexpensive and accurate marker of fibrosis in HCV infection. comparison with liver biopsy and fibrotest. Hepatology. 2007;46:32-6.

18. Jabor A, Kubíček Z, Fraňková S, Šenkeříková R, Franeková J. Enhanced liver fibrosis (ELF) score: Reference ranges, biological variation in healthy subjects, and analytical considerations. Clin Chim Acta. 2018;483:291-95.

19. Gudowska M, Cylwik B, Chrostek L. The role of serum hyaluronic acid determination in the diagnosis of liver fibrosis. Acta Biochim Pol. 2017; 64:451-57.

20. Khan S, Subedi D, U Chowdhury M.M. Use of amino terminal type III procollagen peptide (P3NP) assay in methotrexate therapy for psoriasis, Postgrad Med. J. 2006;82:353-54.

21. Murawaki Y, Ikuta Y, Nishimura Y, Koda M, Kawasaki H. Serum markers for connective tissue turnover in patients with chronic hepatitis B and chronic hepatitis C: A comparative analysis. J Hepatol. 1995;23:145-52.

22. Bulatova I.A, Schekotova A.P, KrivtsovA.V, Schekotov V.V, Pavlov A.I. The noninvasive evaluation of degree of expression of fibrosis of liver and significance of polymorphism of gene of hyaluronic acid under chronic hepatitis C. Klin Lab Diagn. 2015;60:18-21.

**Figure legends**

Fig. 1 Calculation of $^{99m}$Tc-GSA scintigraphy derived indices

a) The $LHL_{15}$ value was calculated by dividing the radioactivity of the liver ROI (solid line) by the sum of the radioactivity of the liver and heart ROIs (solid line and dot line) at 15 min post-injection. The $LHL_{15}$ value lacks the three-dimensional depth direction information.

b) $SUV_{mean}$ was measured by setting the volume of interest at the site of $^{99m}$Tc-GSA accumulation.

Fig. 2 The diagnostic value for severe fibrosis

AUCs were compared in four variables: platelet count, prothrombin time activity, $LHL_{15}$, and $SUV_{mean}$. $SUV_{mean}$ showed the largest AUC.

DH18101　所谷亮太朗

**研究業績リスト**

### 論 文

1. Tokorodani R, Sumiyoshi T, Okabayashi T, et al, Liver fibrosis assessment using $^{99m}$Tc-GSA SPECT/CT fusion imaging. Jpn J Radiol 2019;37(4):315-320.
2. Tokorodani R, Daisaki H, Yukinori O, et al, Effect of position and volume of spaceoccupying liver lesions on liver function index in $^{99m}$Tc-GSA scintigraphy. Nucl Med Rev Cent East Eur. 2021;24(1):1-10.

### 学会発表

1. 所谷亮太朗：$^{99m}$Tc-GSA による新しい肝線維化の指標. 第38回 核医学技術学会総会学術大会，沖縄，2018.
2. 所谷亮太朗：肝受容体シンチグラフィでみる肝臓の線維化. 第76回高知県核医学症例検討会 高知, 2019.
3. 所谷亮太朗：低ペネトレーション高分解能型コリメータを使用したセンチネルリンパ節シンチグラフィの評価. 第35回日本診療放射線技師学術大会, 大宮, 2019.

12

DH18101 所谷亮太朗